CHAPTER 9

INTERPLANETARY FLIGHT

9-1 INTRODUCTION

With the advent of interplanetary flight, man and his machines will break away from "coastal" navigation and venture onto the "high seas" of space flight. If operations in cislunar and lunar space can be likened to the pioneering journeys of Odysseus and other early Greek seafarers, flights into the solar system compare with the accomplishments of the Vikings, the Polynesians, of Columbus, Magellan, and Da Gama. Interplanetary explorers are faced with higher energy requirements, a loneliness never experienced before in the vast space of the solar system which will reduce their home planet to a star or, at times, render it entirely invisible. Above all, they will face much longer flight times which may range from a significant fraction of a year to a significant fraction of their lifetime. *Reduction of flight time is therefore the key problem of manned interplanetary flight.* Without its solution there cannot and will not ever be more than a marginal interplanetary capability, restricting man essentially to the inner solar system with occasional expeditions at great effort. Therewith, our success in interplanetary flight is irrevocably connected with our success in developing adequate propulsion systems which offer the best compromise between sufficiently high acceleration for reducing the mission period to Venus or Mars at least to periods between 0.5 and 1.5 years and as high a specific impulse as possible in order to minimize Earth-to-orbit logistic problems.

9-2 INTERPLANETARY FLIGHT PATHS

In contrast to a transfer between satellites and a lunar transfer, a complete interplanetary transfer consists essentially of three parts

1. Escape from the departure planet
2. Heliocentric transfer
3. Capture by the target planet

The first and the last part involve hyperbolic orbits, whereas the intermediate portion, commonly depicted as a heliocentric ellipse, may also be a heliocentric parabola or hyperbola.

Escape and capture represent only very small sections of the heliocentric transfer path (Fig. 9-1). The space region in which the planet, rather than the Sun, can be regarded as the center body and in which the concept of the hyperbolic flight path holds with good approximation is given by the planet's *activity sphere* which can be approximated by the relation

$$r_{act} = R_{pl}\left(\frac{K_{pl}}{K_{\odot}}\right)^{2/5} \tag{9-1}$$

as was shown in Vol. I of *Space Flight*, Eq. (6-224), p. 479. The mean synodic periods are based on the *mean* angular motions of the planets.

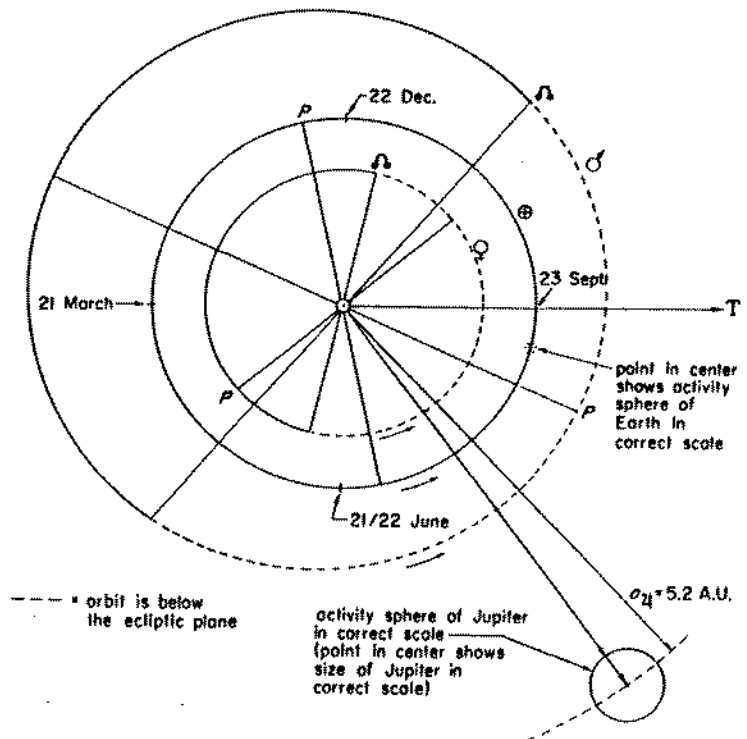

FIG. 9-1 The Orbits of Venus, Earth and Mars in Correct Proportion and Shape With the Activity Spheres of Earth and Jupiter in Correct Scale.

The *actual* synodic periods oscillate around this value, the differences being caused by the variation in angular velocity due to the ellipticity of the planet orbits. For Mars, the actual synodic period varies between $2^y\ 34^d$ and $2^y\ 80^d$. Since 7 synodic periods correspond to nearly 15 years, Mars will appear every 15 years at the same time of the year in opposition to the Sun. The radius of the activity sphere of the planets is listed in

TABLE 9-1a ABBREVIATED TABLE OF PLANETARY CONSTANTS[a]

Planet	Semi-major axis[b] (A.U.)	Perihelion[b] (A.U.)	Aphelion[b] (A.U.)	Eccentricity[b] (—)	Inclination to Ecliptic ° ′ ″	Mean Orbital Velocity[b] (⊕ = 1)	Period of Revolution (Sidereal) (Earth Years)
Mercury	0.387	0.3075	0.4667	0.2056	7 0 14.2	1.6072	0.2411
Venus	0.723	0.7184	0.7282	0.0068	3 23 39.1	1.1758	0.6156
Earth	1.0 = 83.5 · 10⁴ n.m.	0.9833	1.0167	0.0167	—	1.0 = 97,670 ft/sec	1.0 = 365[d].256
Mars	1.524	1.3814	1.6659	0.0934	1 50 50.8	0.8068	1.8822
Jupiter	5.203	4.9508	5.4548	0.0484	1 18 19.9	0.4384	11.86
Saturn	9.539	9.0076	10.0700	0.0557	2 29 42.2	0.3238	29.46
Uranus	19.182	18.2765	20.0873	0.0472	0 46 22.9	0.2283	84.0
Neptune	30.058	29.800	30.3154	0.0086	1 46 26.5	0.1824	164.8
Pluto	39.518	29.6919	49.3436	0.2486	17 8 38.4	0.7591	247.7

Period of Revolution (Sidereal) (in Earth Years)	Mean Synodic Period (Eq. 9-39) Av.[c] Months	Years	Planet Radius (n. mi.)	Activity Sphere[b,c] Planet Radius = 1	n. mi.	km	Solar g-Value at given Major Axis (g⊕)	Solar Constant	Radial Distance $r/r_{\oplus\odot}$ at which Planet's Attraction is 10^{-3} of the Sun's at Planet's Distance
1.515	3.815	0.318	1350	44.6	60,220	$0.11 \cdot 10^8$	$4.01 \cdot 10^{-8}$	6.7	94
3.865	19.2	1.6	3348	99.2	332,160	$0.61 \cdot 10^8$	$1.15 \cdot 10^{-8}$	1.9	273
6.283	—	—	3440	144.9	498,765	$0.92 \cdot 10^8$	$6.10 \cdot 10^{-4}$	1.0 = 1.36 kw/m²	470
11.825	25.6	2.13	1787	174.4	311,627	$0.58 \cdot 10^8$	$2.62 \cdot 10^{-4}$	0.43	400
74.6	13.11	1.093	37,732	640.7	$24.17 \cdot 10^8$	$44.8 \cdot 10^8$	$2.25 \cdot 10^{-4}$	0.04	3535
185.1	12.43	1.035	31,075	743.1	$23.09 \cdot 10^8$	$42.8 \cdot 10^8$	$6.70 \cdot 10^{-4}$	0.01	4460
517.9	12.15	1.012	13,769	2027.4	$27.91 \cdot 10^8$	$51.7 \cdot 10^8$	$1.65 \cdot 10^{-4}$	$3 \cdot 10^{-3}$	7700
1350	12.09	1.007	13,499	3471.6	$46.85 \cdot 10^8$	$86.8 \cdot 10^8$	$6.05 \cdot 10^{-5}$	10^{-3}	13,240
1555	12.05	1.004	(1800)	—	$18.30 \cdot 10^8$	$33.9 \cdot 10^8$	$3.72 \cdot 10^{-5}$	$6 \cdot 10^{-4}$	10,360

[a] For a more extensive list cf. Tables 3-1, Vol. I of *Space Flight*.
[b] Values were rounded off.
[c] Computed from the values given (*loc. cit.* footnote [a]) in Astronomical Units. The value of r_{act} for the Earth applies to the planet only. The activity sphere is only insignificantly enlarged by the Moon. The values, based on the relation r_{act} (A.U.) $= K_{pl}/K_{\odot}$ and using metric values for K yield, for the Earth only, $r_{act} = K_{\oplus}/K_{\odot} = 6.185 \cdot 10^{-3}$ A.U. and for Earth and Moon, $r_{act} = K_{\oplus\mathbb{C}}/K_{\odot} = 6.213 \cdot 10^{-3}$ A.U. corresponding in both cases to about 2.5 Moon distances.
[d] Average month = 365.25/12 ≈ 30.44 day; e.g. for Mercury, $3.815^{mo} = 116.129^{d}$.

Tab. 9-1 together with other basic planetary constants. The activity sphere should not be confused with the sphere within which the planet's gravitational potential perturbs to some relevant degree the heliocentric path of the escaping or approaching spacecraft. The limit of this region around a planet, that is, the degree of perturbative relevance, depends somewhat on the navigational accuracy tolerance involved, but may be taken as the distance where planetary attraction is reduced to 1/50 to 1/100 of local solar gravitational attraction (cf. Tab. 9-1, last column).

In the following discussion of heliocentric transfer orbits, the planetocentric portions will, therefore, be neglected. In order to establish a system for the multitude of heliocentric mission profiles which can be flown, these have been divided in eight elliptic orbits, the parabolic and three hyperbolic transfer orbits. The twelve orbits are listed in Tab. 9-2, and shown in Fig. 9-2a,b. The upper portion of Fig. 9-2a considers transfers from an inner to an outer orbit, the lower portion depicts transfer orbits from an outer to an inner orbit. A one-way elliptic transfer can be identified by a one-digit number (e.g., 0 is the Hohmann transfer), a round trip by a two-digit number (e.g., 00 for the Hohmann mission profile). We will further agree at this point that in a two-digit mission profile the first number identifies the transfer path from Earth to target planet (outgoing transfer), the second number specifies the transfer path from target planet to Earth (return transfer). Where hyperbolic transfers are involved, or in cases where a round trip involves more than one target planet, hence, represents a succession of several transfer orbits, the transfer orbit

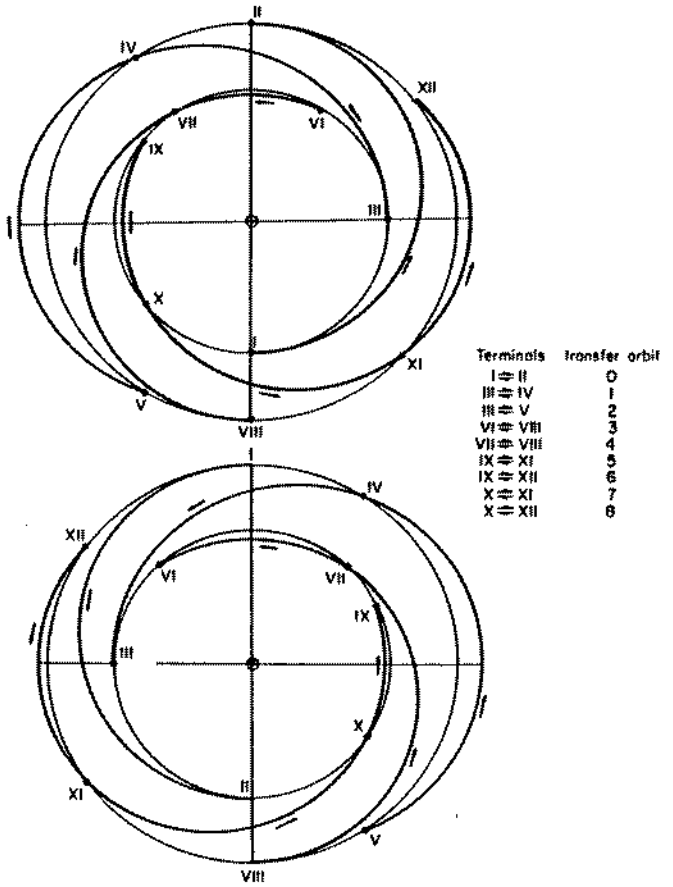

FIG. 9-2a The Nine Basic Types of Elliptic Heliocentric Transfer Orbits.

TABLE 9-1b PLANET VELOCITIES IN VARIOUS UNITS
(Cf. Tab. 9-1 for Earth's Velocity as Unit)

	1			2			3		
	Circular Velocity at Mean Distance			Perihelion Velocity			Aphelion Velocity		
Planet	A.U./sec	km/sec	ft/sec	A.U./sec	km/sec	ft/sec	A.U./sec	km/sec	ft/sec
Mercury	3.2006×10^{-7}	47.8484	156,983	3.9430×10^{-7}	58.9464	193,462	2.5980×10^{-7}	38.8398	127,427
Venus	2.3413×10^{-7}	35.0035	114,843	2.3574×10^{-7}	35.2424	115,624	2.3415×10^{-7}	34.6048	113,533
Earth	1.9913×10^{-7}	29.7701	97,670	2.0078×10^{-7}	30.0	98,385	1.9746×10^{-7}	29.54	96,840
Mars	1.6132×10^{-7}	24.1175	79,103	1.7102×10^{-7}	25.5678	83,884	1.6540×10^{-7}	24.7266	81,124
Jupiter	8.7301×10^{-8}	13.0516	42,820	9.1620×10^{-8}	13.6971	44,938	8.3221×10^{-8}	12.4415	40,818
Saturn	6.4475×10^{-8}	9.6390	31,624	6.8156×10^{-8}	10.1894	33,430	6.0965×10^{-8}	9.1431	29,903
Uranus	4.5467×10^{-8}	6.7715	22,301	4.7666×10^{-8}	7.1260	23,379	4.3369×10^{-8}	6.4836	21,272
Neptune	3.6322×10^{-8}	5.4300	17,815	3.6635×10^{-8}	5.4769	17,969	3.6012×10^{-8}	5.3838	17,663
Pluto	3.1677×10^{-8}	4.7357	15,537	4.0836×10^{-8}	6.1049	20,029	2.4572×10^{-8}	3.6736	12,052

TABLE 9-2 CHARACTERISTICS OF THE ELEVEN BASIC TRANSFER ORBITS (T.O.)

T.O. No.	Terminal Stations	η_t (deg)	Description	
			Inner (Lower) Orbit, R_L	Outer (Upper) Orbit, R_U
0	I ⇌ II	180	$\theta = 0°$; cotangential if coplanar (Hohmann Transfer Ellipse)	$\theta = 0°$; cotangential if coplanar
1	III ⇌ IV	< 180	$\theta = 0°$; $R_P = R_L$ if R_L is circular	$\theta \neq 0°$; $R_A > R_U$; first intersection if R_U is target orbit
2	III ⇌ V	> 180	$\theta = 0°$; $R_P = R_L$ if R_L is circular	$\theta \neq 0°$; $R_A > R_U$; second intersection if R_U is target orbit
3	VI ⇌ VIII	> 180	$\theta \neq 0°$; $R_P < R_L$; second intersection if R_L is target orbit	$\theta = 0$; $R_A = R_U$ if R_U is circular
4	VII ⇌ VIII	< 180	$\theta \neq 0°$; $R_P < R_L$; first intersection if R_L is target orbit	$\theta = 0$; $R_A = R_U$ if R_U is circular
5	IX ⇌ XI	≷ 180	$\theta \neq 0°$; $R_P < R_L$; second intersection if R_L is target orbit	$\theta \neq 0$; $R_A > R_U$; first intersection if R_U is target orbit
6	IX ⇌ XII	> 180	$\theta \neq 0°$; $R_P < R_L$; second intersection if R_L is target orbit	$\theta \neq 0°$; $R_A > R_U$; second intersection if R_U is target orbit
7	X ⇌ XI	< 180	$\theta \neq 0°$; $R_P < R_L$ first intersection if R_L is target orbit	$\theta \neq 0°$; $R_A > R_U$; first intersection if R_U is target orbit
8	X ⇌ XII	≷ 180	$\theta \neq 0°$; $R_P < R_L$; first intersection if R_L is target orbit	$\theta \neq 0°$; $R_A > R_U$; second intersection if R_U is target orbit
9	Parabola	< 180	$\theta = 0°$; $R_P = R_L$ if R_L is circular; $\theta \neq 0°$	$\theta \neq 0°$
10	XIII ⇌ XIV	< 180	$\theta = 0°$; $R_P = R_L$ if R_L is circular	$\theta \neq 0°$
11	XV ⇌ XVII	< 180	$\theta \neq 0°$; $R_P < R_L$; first intersection if R_L is target orbit	$\theta \neq 0°$
12	XVI ⇌ XVII	< 180	$\theta \neq 0°$; $R_P < R_L$; second intersection if R_L is target orbit	$\theta \neq 0°$

numbers should be separated by commas, again counting from Earth back to Earth.

The transfer orbit classification presented in Fig. 9-2a,b is perfectly general and independent of ellipticity and inclination of the planet orbits or any other departure and target orbit. The effects of ellipticity and inclination will be treated in later paragraphs.

9-3 HOHMANN TRANSFER BETWEEN CO-PLANAR CIRCULAR PLANET ORBITS

This obviously represents an idealized case. The fact that it allows considerable simplifications without seriously compromising the performance spectrum of most transfer maneuvers has made this approach the historical starting point of systematic interplanetary mission computations with Hohmann's first comprehensive study [Ref. (*1*)]. Therefore the Class 0 transfer orbit (Fig. 9-2a) has been named in his honor.

Subsequently, the *Hohmann transfer* will be analyzed first. The equations involved are well known to the reader of this book and Vol. I of *Space Flight* and will therefore be summarized here without further explanation. The transfer nomenclature is presented in Fig. 9-3. All other symbols used have been explained many times before and are also summarized in the list of principal notations at the end of this chapter. Although the escape and capture orbits will not be considered, the *energy requirement* for escape and capture will be included in the analysis of this

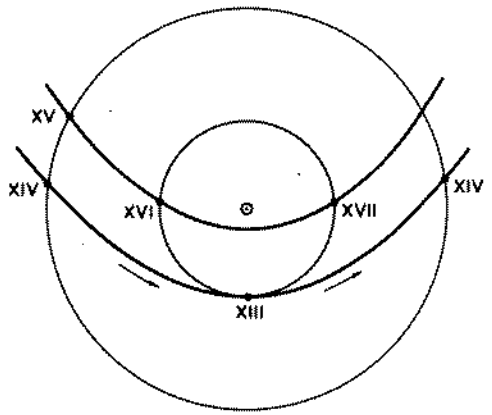

Terminals	Transfer orbit
XIII ⇌ XIV	10
XV ⇌ XVI	11
XV ⇌ XVII	12

FIG. 9-2b The Three Basic Types of Hyperbolic Transfer Orbits.

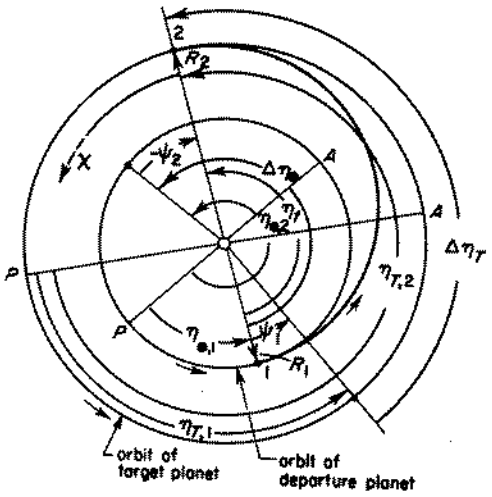

P = perihelion
A = aphelion
R = heliocentric distance
η = true anomaly
$\Delta\eta_D, \Delta\eta_T$ = center angle covered by departure and target planet during transfer period
η_f = center angle covered by spacecraft during transfer period
ψ = position angle of target planet with respect to target planet
χ = center angle covered during capture period of spacecraft as satellite of target planet

(Positive angles are measured counter - clockwise)
Subscripts:
D = departure planet
T = target planet
S = spacecraft
1 = departure point
2 = arrival (target) point
f = transfer

FIG. 9-3 Nomenclature of Heliocentric Transfer.

paragraph. However, the effect of eccentricity and inclination of the planet orbits and of the required transfer orbit inclination on the transfer energy requirement will be neglected here. It is reserved for a discussion in Par. 9-4.

Heliocentric departure velocity

Transfer to an *outer planet.*

$$\frac{V_1}{\sqrt{K_\odot/R_P}} = V^*_1 = V^*_P = \sqrt{1+\frac{n-1}{n+1}} \tag{9-2}$$

where $n = R_A/R_P$ and $\sqrt{K_\odot/R_P} = \sqrt{K_\odot/a_\oplus}$, $a_\oplus$ being the semi-major axis of the Earth's orbit.

Transfer to an *inner planet.*

$$V^*_1 = V^*_A = \sqrt{1-\frac{n-1}{n+1}} \tag{9-3}$$

where $V^*_A = \sqrt{K_\odot/R_A} = \sqrt{K_\odot/a_\oplus}$.

Since in a Hohmann maneuver the departure and arrival are cotangential, it follows

$$V^*_1 - 1 \pm \Delta V^*_1 = v^*_\infty \tag{9-4}$$

so that, for transfer to an outer or inner planet, respectively, it follows
Planetocentric escape velocity

$$v^*_{h,1} = \sqrt{v^{*2}_p + v^{*2}_{\infty,1}} \tag{9-5}$$

or, for departure from a circular satellite orbit

$$\Delta v^*_{h,1} = v^*_{h,1} - v^*_c = v^*_{h,1} - \frac{1}{U_\oplus}\sqrt{K_\oplus / r_1} \tag{9-6}$$

Here the asterisk means, like for the capital letter heliocentric velocities, that they are put in nondimensional form by division by the mean velocity of the Earth

$$U_\oplus = V_{c,a_\oplus} = \sqrt{K_\odot / a_\oplus} = V_{c,\oplus} \tag{9-7}$$

It is convenient to carry out interplanetary transfer computations in terms of the mean Earth velocity and of the astronomical unit as unit of length. If, in addition, the unit of time is taken as $1/(2\pi)$ years, it follows $V_{c,\oplus} = 1$ and $K_\odot = 1$. This is very useful for intermediate computations or for electronic computer analyses, but the final result is difficult and cumbersome to use if presented in these units. Table 9-1b lists the mean velocity as well as the apsidal velocities of all planets in terms of A.U./sec, km/sec and ft/sec, whereas in Tab. 9-1a the velocities are given in terms of the Earth's mean velocity.

Assuming the spacecraft departs from the vertex of the hyperbola, the *escape period* to a distance r_{sct} (limit of the activity sphere) follows from the following equations

$$e = 1 + \frac{v^2_{\infty,1}}{K_\oplus / r_P} = 1 + \frac{v^{*2}_{\infty,1}}{v^{*2}_c} \tag{9-8}$$

$$a = \frac{K_\oplus}{v^2_{\infty,1}} \tag{9-9}$$

$$\cos H = \frac{e}{1 + \frac{r_{sct}}{a}} \tag{9-10}$$

$$M = e \tan H - \ln \tan\left(45° + \frac{H}{2}\right) \tag{9-11}$$

$$t_{Pr_{sct}} = M\sqrt{\frac{a^3}{K_\oplus}} \tag{9-12}$$

Asymptote half angle of the escape hyperbola

$$\cos\phi = \frac{1}{e} \tag{9-13}$$

The *turning angle* between geocentric hyperbolic departure direction and geocentric direction at heliocentric departure (asymptote) after escape is [cf. Eq. (4-27)] equal to one-half the over-all turning angle ζ at a hyperbolic encounter,

$$\tfrac{1}{2}\Delta\zeta = 90 - \phi = \sin^{-1}\frac{1}{e} \tag{9-14}$$

The *heliocentric transfer time* for the half-ellipse shaped transfer orbit is easily computed from

$$t_t = \pi\sqrt{\frac{a^3(\text{A.U.})^3}{K_\odot[(\text{A.U.})^3/\text{sec}^2]}}\ (\text{sec}) \tag{9-15}$$

with

$$a = \tfrac{1}{2}(R_A + R_P)\ (\text{A.U.}) \tag{9-16}$$

$$K_\odot = 3.96529 \cdot 10^{-14}\ [(\text{A.U.})^3/\text{sec}^2] \tag{9-17}$$

The center angle covered by Earth and target planet (pl) during the transfer is therefore (Fig. 9-3),

$$\Delta\eta_\oplus = \mu_\oplus t_t \tag{9-18}$$

$$\Delta\eta_{pl} = \mu_{pl} t_t \tag{9-19}$$

The departure position angle of the target planet follows to be

$$\psi_1 = \eta_t - \Delta\eta_{pl} = 180° - \Delta\eta_{pl} \tag{9-20}$$

and the arrival constellation

$$\psi_2 = \Delta\eta_\oplus - \eta_t = \Delta\eta_\oplus - 180° \tag{9-21}$$

The last expressions on the right-hand side of Eq. (9-20) and (9-21) apply to Hohmann transfers only. Equations (9-20) and (9-21) are based on the rule, set here, that ψ_1 = positive means that the target planet is "ahead" of the Earth, ψ_2 = positive means that Earth is ahead of target planet.
Heliocentric arrival velocity is for transfer to an outer planet

$$V^*_2 = V^*_A = V^*_P \frac{R_P}{R_A} \tag{9-22}$$

and for transfer to an inner planet

$$V^*_2 = V^*_P = V^*_A \frac{R_A}{R_P} \tag{9-23}$$

The *heliocentric arrival velocity difference* is therefore

$$\Delta V_2 = v_{\infty,2} = V_P - \sqrt{K_\odot/a_{pl}} \quad \left.\right\} \text{Transfer to an inner orbit} \qquad (9\text{-}24a)$$

$$\Delta V^*_2 = v^*_{\infty,2} = V^*_P - \sqrt{\frac{1}{a^*_{pl}}} \quad \left.\right\} \text{Transfer to an inner orbit} \qquad (9\text{-}24b)$$

$$\Delta V_2 = v_{\infty,2} = \sqrt{K_\odot/a_{pl}} - V_A \quad \left.\right\} \text{Transfer to an outer orbit} \qquad (9\text{-}25a)$$

$$\Delta V^*_2 = v^*_{\infty,2} = \sqrt{\frac{1}{a^*_{pl}}} - V^*_A \quad \left.\right\} \text{Transfer to an outer orbit} \qquad (9\text{-}25b)$$

The *capture energy requirement* depends on the capture maneuver, the altitude and the eccentricity of the capture orbit. A single-impulse maneuver, changing the orbit from hyperbola to an elongated ellipse requires the least amount of energy. A two-impulse maneuver into a circular satellite orbit (cf. Chap. 4) is more expensive, but under certain conditions still more economical than a single-impulse orbit change from hyperbola to circle. The minimum energy requirement for the latter maneuver is (cf. Chap. 4)

$$\Delta v_{h,2} = \sqrt{\frac{2K_{pl}}{\bar{r}}} - \sqrt{\frac{K_{pl}}{\bar{r}}}$$

where $\bar{r}$ is given for each planet in Tab. 4-1 and also Tab. 9-3 below. In

TABLE 9-3 AUXILIARY DATA FOR TYPICAL STANDARD CAPTURE AND ESCAPE DISTANCES

		Minimum 1—Impulse Maneuver			Maneuver at 1.1 Planet Radius		
Planet	K_{pl} (n. mi.^{3}/sec^2)	$\bar{r}$ (n. mi.)	$\bar{v}_c$ (ft/sec)	$\bar{v}_p$ (ft/sec)	1.1 r_{00} (n. mi.)	$(v_c)_{1.1r_{00}}$ (ft/sec)	$(v_p)_{1.1r_{00}}$ (ft/sec)
Mercury	3408	(208)	(24,900)	(35,200)	1490	9200	13,010
Venus	51,041	48,100	6260	8760	3680	22,610	32,000
Mars	6754	7050	5940	8850	1965	11,260	15,920
Jupiter	$19.914 \cdot 10^6$	4,265,000	13,130	18,550	41,500	133,100	188,000
Saturn	$5.963 \cdot 10^6$	1,291,000	13,060	18,460	34,200	80,200	114,400
Uranus	$0.91207 \cdot 10^6$	280,000	10,960	15,500	15,100	39,500	66,700
Neptune	$1.08 \cdot 10^6$	433,000	9600	13,560	14,850	51,800	73,200
Pluto	52,146	3000	25,300	35,800	2000	23,400	32,800

comparison, a single-impulse maneuver for change into an elliptic orbit at an arbitrary distance, say, $r_P = 1.1 r_{00}$ where r_{00} is the radius of the planet, follows from the following relations,

$$a = \frac{K_{pl}}{v_{\infty,2}^2} \qquad (9\text{-}26)$$

$$v_P = v_{h,2} = \sqrt{\frac{2K_{pl}}{r_P} + v_{\infty,2}^2} \qquad (9\text{-}27)$$

$$\tan\phi = \frac{v_P v_{\infty,2}}{K_{pl}/r_P} \qquad (9\text{-}28)$$

$$e = \sec\phi \qquad (9\text{-}29)$$

$$\Delta v_{h,2} = v_{h,2} - v_{P,\,capture} \qquad (9\text{-}30a)$$

where $v_{P,\,capture}$ is the peri-apsis velocity of the capture orbit. If this orbit is a circle, $r_P = r_c$,

$$\Delta v_{h,2} = v_{h,2} - \sqrt{K_{pl}/r_c} \qquad (9\text{-}30b)$$

The *departure position angle* for return along a Hohmann orbit is given by

$$\psi_3 = \eta_t - \Delta\eta_\oplus = -\psi_2 \qquad (9\text{-}31)$$

Consequently, the capture period, i.e., stay time near the target planet,

$$t_{cpt} = \frac{360 - 2\psi_3}{|\mu_\oplus - \mu_{pl}|} \qquad (9\text{-}32)$$

The Hohmann return flight is a repetition in reverse of the outgoing flight. The mission velocity becomes therefore

$$\Delta v_{tot} = \Delta v_{h,1} + 2\Delta v_{h,2} + \Delta v_{h,4} \qquad (9\text{-}33)$$

if different Earth satellite orbits are used for departure and return, or

$$\Delta v_{tot} = 2(\Delta v_{h,1} + \Delta v_{h,2}) \qquad (9\text{-}34)$$

if identical satellite orbits are assumed.

Table 9-3 presents auxiliary data for typical standard capture and escape distances. Tables 9-4 and 9-5 summarize the essential orbital and

TABLE 9-4 HOHMANN TRANSFER ORBITS FROM EARTH TO TARGET PLANET: BASIC DATA OF TRANSFER ORBIT Nr. 0

Target Planet	e_t[a]	Heliocentric Target Distance	Velocity at Target (Departure Velocity = 1)
Mercury	0.44	0.38709	2.58331
Venus	0.16	0.72333	1.38249
Mars	0.20	1.52369	0.65630
Jupiter	0.67	5.20280	0.19220
Saturn	0.81	9.53884	0.10483
Uranus	0.90	19.18196	0.05213
Neptune	0.93	30.05773	0.03326
Pluto	0.95	39.51774	0.02530

[a] e_t = eccentricity of heliocentric Hohmann transfer orbit (transfer orbit Nr. 0).

TABLE 9-5 HOHMANN TRANSFER ORBITS: VELOCITY DATA IN TERMS OF THE EARTH'S MEAN ORBITAL VELOCITY

Heliocentric Data							Planetocentric Data								
Hohmann Transfer between Circular, Co-planar Planet Orbits							Minimum 1-Impulse Circular Orbit						Circular Orbit at 1.1 Planet Radius		
Target Planet	R (A.U.)	U^*_{pl}	V^*_1	V^*_2	$\Delta V^*_1 = v^*_{\infty,1}$	$\Delta V^*_2 = v^*_{\infty,2}$	ΔV^*_{tot}	$v^*_{h,1}$	$v^*_{h,2}$	Δv^*_1	Δv^*_2	Δv^*_{tot}	Δv^*_1	Δv^*_2	Δv^*_{tot}
Mercury	0.387	1.607	0.7471	1.931	−0.2529	0.324	0.5769	0.4401	(0.4401)	0.1852	(0.229)	(0.8271)	0.1849	0.2525	0.8748
Venus	0.723	1.176	0.9162	1.268	−0.0838	0.092	0.1758	0.3695	0.3695	0.1151	0.0651	0.3602	0.1150	0.1860	0.602
Earth	1.000	1.000	—	—	—	—	—	—	—	—	—	—	—	—	—
Mars	1.523	0.8068	1.0989	0.7210	0.0989	0.0858	0.1847	0.3734	0.3734	0.1185	0.0606	0.3582	0.1184	0.0703	0.3774
Jupiter	5.2	0.4384	1.259	0.2540	0.259	0.1844	0.4434	0.4656	0.4656	0.2112	0.1304	0.6832	0.2109	0.5730	1.5678
Saturn	9.54	0.3238	1.345	0.1410	0.345	0.1828	0.5278	0.4978	0.4988	0.2439	0.1291	0.7460	0.2432	0.3515	1.1894
Uranus	19.18	0.2283	1.379	0.0719	0.379	0.1564	0.5354	0.5226	0.5226	0.2705	0.1108	0.7626	0.2703	0.2215	0.9836
Neptune	30.06	0.1824	1.390	0.0462	0.390	0.1362	0.5262	0.5307	0.5307	0.278	0.0965	0.749	0.2779	0.2489	1.0536
Pluto	39.52	0.1591	1.396	0.0354	0.396	0.1237	0.5197	0.5352	0.5352	0.2822	0.0875	0.7394	0.282	0.1622	0.8884
Parabolic	∞	0	1.414	0	0.414	0	0.414	0.5470	0	0.2921	0	0.2921	—	—	—
Sun-Center	0	—	0	∞	1.000	—	1.000	1.0630	∞	0.8081	0	0.8081	—	—	—

Earth escape conditions: $y = 300$ n. mi.; $v_c = 24{,}900$ ft/sec; $U_\oplus = 97{,}670$ ft/sec; $v^*_c = 0.2549$; $v^*_p = 35{,}200$ ft/sec; $v^*_p = 0.36$; $(v^*_p)^2 = 0.1296$; $\Delta v^*_1 = v^*_{h,1} - v^*_c$.

Planet capture conditions: Optimum 1-impulse capture in circular satellite orbit: $\Delta \bar{v} = \sqrt{K/\bar{r}} = v^*_{\infty,pl}/\sqrt{2} = \Delta v^*_{pl}$; $\Delta v^*_{tot} = 2(\Delta v^*_1 + \Delta v^*_2)$; $\Delta V^*_{tot} = \Delta V^*_1 + \Delta V^*_2$.

TABLE 9-6 HOHMANN TRANSFER ORBITS: TIME AND POSITION DATA

Planet	μ_{pl} (deg/day)	t_t (days)	t_t (years)	$\Delta\eta_\oplus$ (deg)	$\Delta\eta_{pl}$ (deg)	η_t (deg)	ϕ_1 (deg)	ϕ_2 (deg)	ϕ_3 deg	t_{cpt} (days)	$T = 2t_t + t_{cpt}$ (days)	$T = 2t_t + t_{cpt}$ (years)
Mercury	4.092	105.5	0.2887	104	432	180	−252	−76	76	67	278	0.772
Venus	1.602	146	0.3999	144	234	180	−54	−36	36	468		2.08
Earth	0.986	—	—	—	—	—	—	—	—	—	—	—
Mars	0.524	258.8	0.7086	255	136	180	44.4	75	−75	455	—	2.66
Jupiter	0.083	997.3	2.731	(2) + 263°	82.8	180	97.2	83	−83	214	—	6.05
Saturn	0.0335	2,208.7	6.05	(6) + 18°	74	180	106	−162	162	341	—	13.03
Uranus	0.0117	5,853.3	16.03	(16) + 11°	68.5	180	111.5	−169	169	346	—	32.998
Neptune	0.006	11,174	30.6	(30) + 218°	66.8	180	113.2	38	−38	292	—	61.98
Pluto	0.004	16,650	45.6	(45) + 217°	66.6	180	113.3	37	−37	291	—	91.97

velocity data for Hohmann transfer between Earth and all other planets in the solar system. The last two lines show, for reason of comparison, the data for a heliocentric escape mission and for radial fall toward the Sun. The heliocentric round-trip mission velocities

$$\Delta V^*_{tot} = |\Delta V^*_1 + \Delta V^*_2| \tag{9-35}$$

to the planets show the characteristic pattern (cf. Chap. 3) of reaching a maximum at 15.8 A.U., that is, between Saturn and Uranus. This pattern is distorted, but nevertheless recognizable for the combined planetocentric and heliocentric maneuvers,

$$\Delta v^*_{tot} = 2(\Delta v^*_1 + \Delta v^*_2) \tag{9-36}$$

The geocentric maneuvers are based on departure from, and return to, a 300 n. mi. circular orbit. The planetocentric maneuvers at the target planet are uniformly based on minimum single-impulse capture in the corresponding circular orbit, i.e., on the lowest energy requirement possible for capture in a circular orbit with one impulse and, secondly, on a circular orbit at 1.1 the planet's radius. It will be remembered from Par. 4-4 that (a bar designates minimum 1-impulse conditions for circular capture orbit), for any planet pl,

$$\bar{v}_h = \sqrt{2}\bar{v}_p = 2\sqrt{K_{pl}/\bar{r}} \tag{9-37a}$$

$$\bar{v}_\infty = \bar{v}_p = \sqrt{2K_{pl}/\bar{r}} \tag{9-37b}$$

$$\Delta v = v_h - \sqrt{K_{pl}/r} \tag{9-37c}$$

so that

$$\Delta\bar{v} = \bar{v}_h - \sqrt{K_{pl}/\bar{r}} = \sqrt{K_{pl}/\bar{r}} = \frac{\bar{v}_\infty}{\sqrt{2}} \tag{9-37d}$$

Therefore, in Tab. 9-3

$$\Delta v^*_2 = \Delta\bar{v}^*_2 = \frac{v^*_{\infty,2}}{\sqrt{2}} \tag{9-38}$$

For Mercury, this capture maneuver is not feasible, since the optimum 1-impulse distance is $\bar{r} < r_{00,\,\mathrm{☿}}$. Therefore, the respective values are put in parenthesis.

The last three columns in Tab. 9-5 summarize the velocity requirement for escape and capture at Earth and target planet at a distance of $1.1 r_{00}$. The mission velocity $\Delta v^*_{\mathrm{tot}}$ is seen to be considerably higher than for the minimum 1-impulse case, especially for the major planets. Tab. 9-6 summarizes the associated data on position, flight time and mission period T.

Figure 9-4 summarizes the energy requirements for lunar flights and for 1-way missions to various places throughout the entire solar system. The value Δv_{tot} given at the ordinate indicates the ideal velocity required for all velocity changes, starting from a satellite orbit at 300 n. mi. altitude. The circular velocity at this altitude is 24,900 ft/sec. The ideal velocity with respect to inertial space required to reach this orbit is about 29,500 ft/sec for large vehicles ascending from the surface at about 1.5 g initial acceleration. For eastward ascent within $\pm 23.5°$ latitude, at least 1300 ft/sec can be subtracted due to Earth rotation. The ideal velocity with respect to the $\pm 23.5°$ belt of the Earth's surface, required to attain circular velocity at 300 n. mi. altitude is therefore $v_d = 28{,}200$ ft/sec. By adding this sum to Δv_{tot} in Fig. 9-4 one obtains very closely the ideal

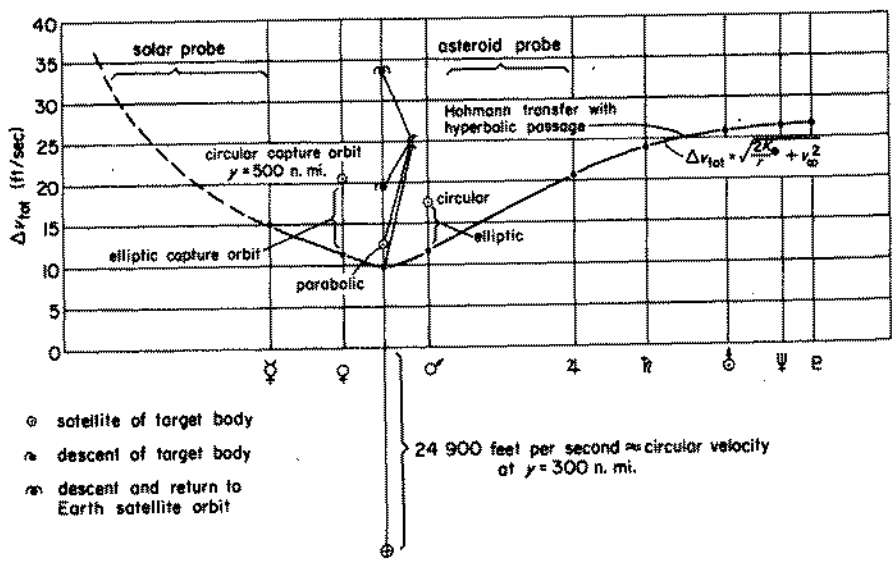

FIG. 9-4 Velocity Requirements for Space Vehicles Launched from a 300 n. mi. High Earth Satellite Orbit (Circular Co-planar Planet Orbits; Hohmann Transfer).

velocity for which an Earth-launched probe must be laid out to accomplish its particular mission. For all planets the hyperbolic passage for co-planar Hohmann transfer is indicated by a curve. The maximum values for circumplanetary capture (namely, in a circular satellite orbit) are indicated for Venus and Mars, at a capture altitude of 2000 n. mi. for Venus and 6000 n. mi. for Mars. From this value on downward, until planetocentric parabolic velocity is reached, lies the region of elliptic capture orbits. It may be noted that even 1-way landing operations on the Moon are more expensive than minimum-energy 1-way nonlanding and (most) capture operations in the entire inner solar system. It should also be noted that for $\Delta v_{\mathrm{tot}} = 28{,}000$ ft/sec all planets of the solar system can be visited by 1-way probes if launched from a satellite orbit. A $\Delta v_{\mathrm{tot}} = 28{,}000$ ft/sec corresponds approximately to the ideal velocity of a

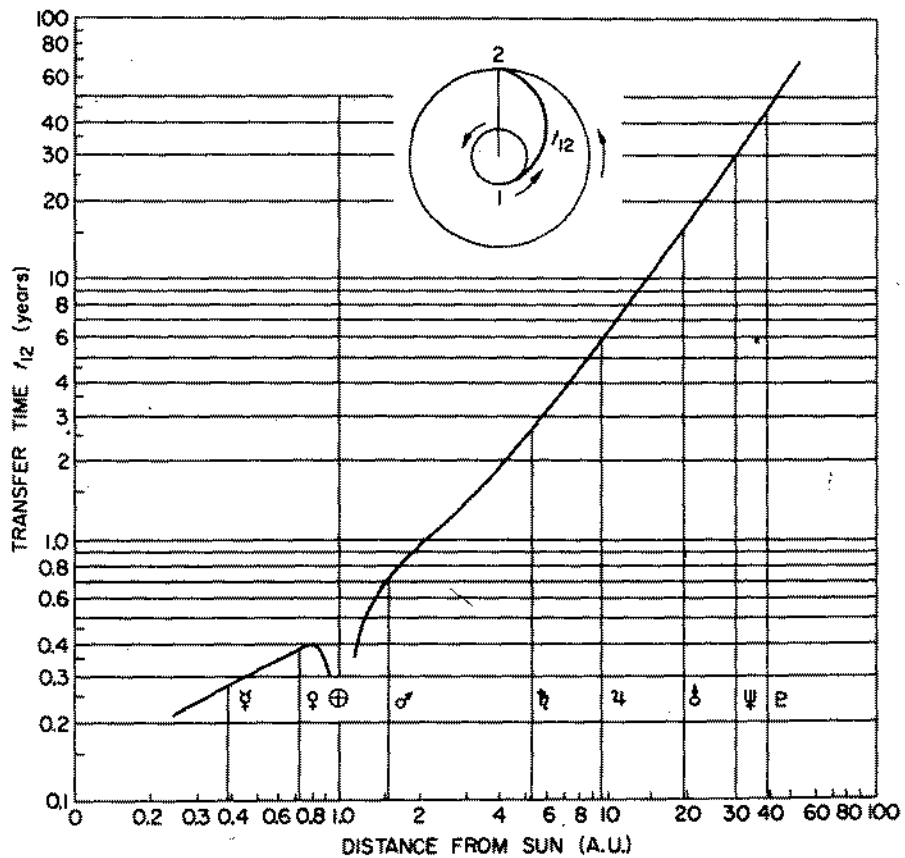

FIG. 9-5 Transfer Time between Earth and Target Planet, Assuming Circular Co-planar Orbits, at Mean Planet Distance and Hohmann Transfer Orbits.

5500 n. mi. ICBM. In practice, however, the transfer time in minimum-energy transfer orbits, which is shown in Fig. 9-5, will limit the transfer of instrumented probes to Jupiter, and even there one will attempt to use faster transfer orbits (for reasons of communication, tracking and limitations in operational life of the payload) as will be discussed in the subsequent paragraph.

Finally, Fig. 9-6 correlates mission period and mission velocity for 2-way missions along Hohmann transfer orbits. The curve represents the variation of heliocentric velocity for transfer from one heliocentric circular orbit to another. The individual points in circles represent the combination of heliocentric and planetocentric transfer energy, departure and arrival orbit at Earth being at 300 n. mi. altitude, departure and arrival orbit at the target planet being the one for minimum 1-impulse capture requirement in a circular orbit. The individual points in triangles represent the effect of departure and arrival at circular orbits at

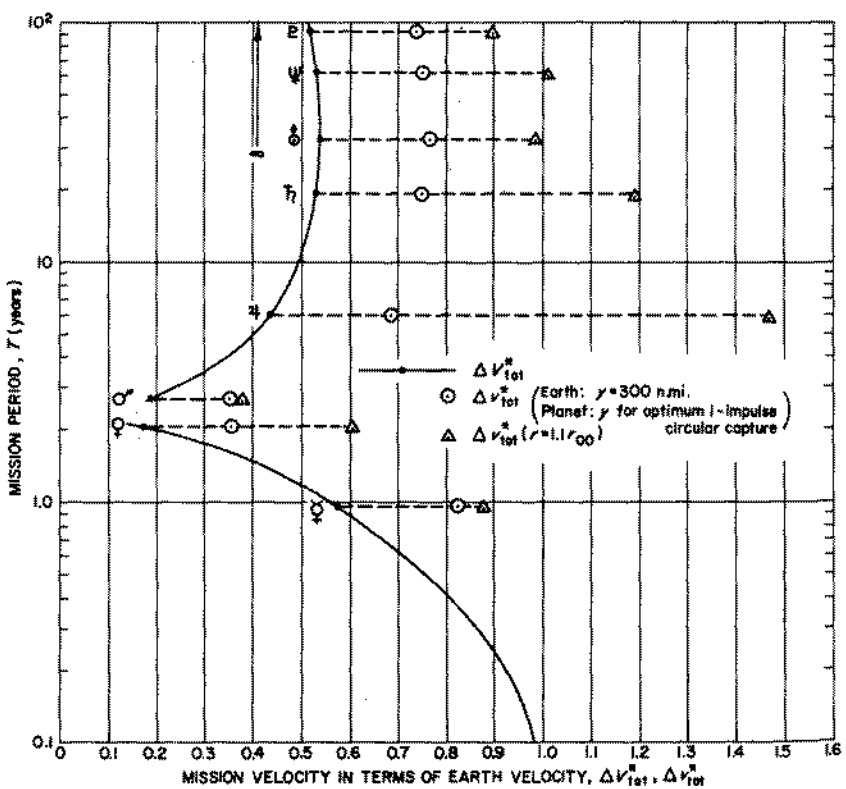

FIG. 9-6 Period and Total Velocity of Interplanetary Round-Trip Missions with Hohmann Transfer.

1.1 r_{00} distance from Earth as well as target planet. The constellational requirements for Earth and target planet in minimum energy transfer are the reason for the very long stay times near the target planets of the inner solar system. These periods are of the same order as the transfer period both ways (Mars) or even larger (Venus). They result in total mission periods of 2 years (Venus), 2.68 years (Mars).

For any given transfer path the flight schedule to another planet is rigidly determined by constellational requirements. This means that the position of Earth and target planet at the time the spacecraft leaves the Earth must be such that planet and spacecraft meet when the latter arrives at the planet's orbit. A given position between Earth and target planet occurs in the average once within a given time period (synodic period) which is given by the relation

$$T_{syn} = \frac{1}{\left|1 - \frac{1}{T_{pl}}\right|} \tag{9-39}$$

where T_{pl} is the sidereal period of the planet in Earth years. The synodic periods with respect to the Earth are presented in Tab. 9-1. Orbital ellipticity and inclination together cause the transfer conditions to vary from one constellation to the next (cf. Par. 9-7). This means that the minimum hyperbolic energy level for injection into the heliocentric transfer orbit varies and that the period between two minimum energy levels may be different from the synodic period. This is illustrated numerically in Tab. 9-7a, in which the Hohmann transfer conditions between coplanar circular planet orbits are compared with the approximate minimum energy transfer conditions between the actual orbits of Earth, Venus and Mars. The time intervals between the actual minimum energy launch dates fluctuate about the synodic period. The fluctuations are larger for Mars as target planet than for Venus, because of the larger eccentricity of the Martian orbit. The differences in hyperbolic excess energy or velocity are seen to vary considerably for each target planet; the variation exceeds the difference between the Hohmann transfer energy to Venus and to Mars. These variations in energy are tied to the variation in heliocentric longitude of the departure point relative to one of the nodes of the target orbit with the Earth orbit. For example, a particularly favorable transfer constellation to Venus offered itself in 1959, permitting a coplanar transfer from node to node of almost 180° transfer angle, a condition approaching Hohmann transfer conditions particularly closely (cf. Fig. 9-61). During the subsequent constellations the departure point moves away from the node, leading to steadily increasing energy requirements during the launch dates from 1961 through 1964. As the opposite node is approached most closely (but not quite as closely as in 1959) in

TABLE 9-7a COMPARISON OF HOHMANN TRANSFER WITH MINIMUM TRANSFER CONDITIONS BETWEEN ACTUAL PLANET ORBITS DURING THE 1960–1971 PERIOD

Earth → Venus	Hohmann	1961	1962	1964	1965	1967	1969
Date of min. energy transf.	—	Jan. 11	Aug. 22	March 29	Nov. 13	June 11	Jan. 3
Synodic recurrence[a]	584.45 days	0	Aug. 18	March 24	Oct. 29	June 7	Jan. 12
$v_{\infty,\min}$ (ft/sec)	8185	9000	9660	11,940	11,400	8426	9500
$h_{min} = v_{\infty}^2{}_{,\min}$ (ft²/sec²)	$0.67 \cdot 10^8$	$0.81 \cdot 10^8$	$0.933 \cdot 10^8$	$1.32 \cdot 10^8$	$1.3 \cdot 10^8$	$0.71 \cdot 10^8$	$0.902 \cdot 10^8$
Transfer time (days)	146	130	120	112	110	142	140
Helioc. transfer angle (deg.)	180	159	141	127	134	176	168
Earth → Mars	**Hohmann**	**1960**	**1962**	**1964**	**1967**	**1969**	**1971**
Date of min energy transf.	—	Sept. 30	Oct. 29	Nov. 21	Jan. 3	**Feb. 28**	**May 22**
Synodic recurrence	779.2	0	Nov. 19	Jan. 7 (65)	Feb. 16	**March 28**	**May 15**
$v_{\infty,\min}$ (ft/sec)	8986	14,300	11,900	9800	9800	**9700**	9300
$h_{min} = v_{\infty}^2{}_{,\min}$ (ft²/sec²)	$0.807 \cdot 10^8$	$2.04 \cdot 10^8$	$1.42 \cdot 10^8$	$0.96 \cdot 10^8$	$0.96 \cdot 10^8$	$0.941 \cdot 10^8$	$0.865 \cdot 10^8$
Transfer time (days	258.8	200	232	240	202	176	209
Helioc. transfer angle (deg.)	180	140	160	124	152	136	155

[a] Defines the dates of launch into a Hohmann transfer orbit if planet orbits were circular and co-planar, counting from Jan. 11, 1961 for Venus and Oct. 5, 1960 for Mars.

1967 the energy is a minimum and thereafter climbs again. The longitude of the ascending node of Venus is about 76°. The Earth, therefore, passes the ascending node approximately 76 deg/30 (deg/mo) $\simeq 2.5$ months after 21 September when the Earth passes through the vernal equinox (Sun in autumnal equinox), i.e., in early December. The descending node is passed in early June. These are, therefore, favorable months for co-planar or near-co-planar transfers to Venus. The corresponding months for tranfers to Mars are early November and early May. Whenever the launch date falls in any of these time periods, the transfer energy is seen to be comparatively low. Further discussion of the effect of orbit eccentricity and inclination is presented in Par. 9-5. The transfer angles are in all cases considerably smaller than 180°. This too is caused by the eccentricity and inclination of the planet orbits. It is also possible to fly along transfer orbits with transfer angles in excess of 180° (cf. Par. 9-5) and these frequently require less transfer energy than the most economical short transfer orbit. However, those orbits have a number of practical disadvantages which include greater error sensitivity and greater distance between Earth and target planet at arrival of the space vehicle.

It is not sufficient, however, to gear interplanetary transfer missions only with respect to minimum energy requirements, since this would offer only an exceedingly small period, namely, nominally one day, in which the space vehicle would have to be launched (*launch window*). This concept is not realistic anyway, since the minimum energy varies so much from one launch constellation to another that the minimum energy for one constellation would offer a comparatively wide launch window for another. Figures 9-46 ff. illustrate this broadening of the launch window with increasing hyperbolic excess, since the launch window is the time period between the descending and the ascending branch of a curve representing a particular transfer period, or between the extreme branches of a group of curves bracketing a suitable range of transfer periods. Figures 9-7 and 9-8 illustrate more specifically the opening up of the launch window for Earth-Venus and Earth-Mars transfers during a number of appropriate constellations in the 1960–70 period. These figures cover a much wider range of hyperbolic excess energy than will be attainable to the first interplanetary launch vehicles (Atlas/Centaur and Saturn). It is seen that for launch windows of the order of 1–2 months, a hyperbolic excess energy level of the order of $1.6 \cdot 10^8$ ft²/sec² is required. Table 9-7b shows the launch schedule for Mercury, Venus, Mars, Jupiter and Saturn, based on 2–3 weeks launch windows for Mercury and approximately two months launch windows for the other planets. The transfer periods which correspond to these launch windows are indicated in the second column of Tab. 9-7b.

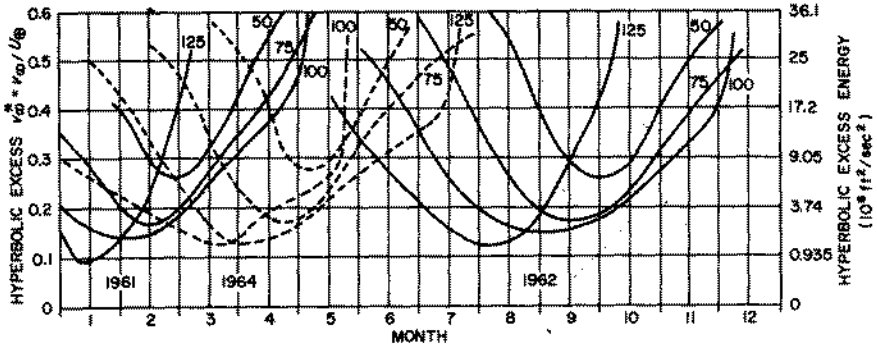

FIG. 9-7 Variation of Launch Window to Venus as Function of Hyperbolic Excess Velocity (numbers on curves designate transfer time in days).

The launch windows can be widened considerably if the following two conditions can be accepted:

(a) The transfer energy is very high and the capture maneuver, therefore, still higher;
(b) Planet and probe meet at very great distance from the Earth, rendering radar and/or optical tracking and data transmission extremely difficult, if not impossible.

Figure 9-9 provides a few illustrations of possible transfer orbits at different departure times, leading to greatly differing arrival distances from the Earth, as well as different energy requirements, accuracy tolerances and transfer periods. Differences in transfer periods can have practical significance in terms of the battery life, fluid storage and probability of damage by meteoritic material. Orbit (A) from Earth to Mars is

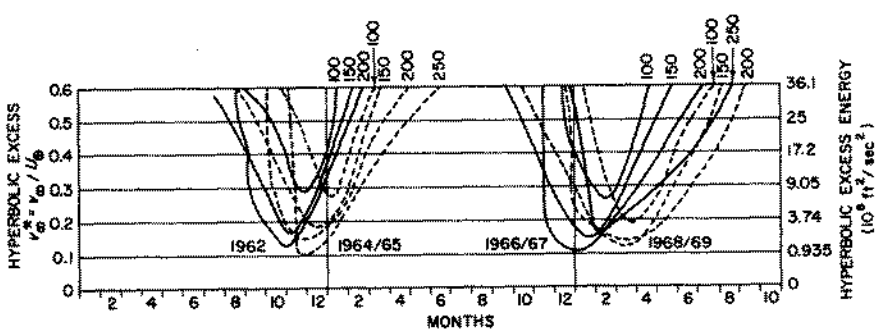

FIG. 9-8 Variation of Launch Window to Mars as Function of Hyperbolic Excess Velocity (numbers on curves designate transfer time in days).

TABLE 9-7b Launch Schedule for Flights to Mercury, Venus, Mars, Jupiter and Saturn.

Planet	Trans. Period	1959	60	61	62	63
		1 Apr 1 July 1 Oct				
Venus	3-4 months					
Mars	7-8 months					
		64	65	66	67	68
Mercury	~ 3 months					
Venus	3-4 months					
Mars	7-8 months					
Jupiter	2-2.1 years					
Saturn	2.5-3 years					
		69	70	71	72	73
Mercury	~ 3 months					
Venus	3-4 months					
Mars	7-8 months					
Jupiter	2-2.1 years					
Saturn	2.5-3 years					

a close approximation (primarily due to the ellipticity of the Mars orbit) of a Hohmann transfer to Mars and therefore is close to minimum energy requirement. However, due to the length of the transfer period, the

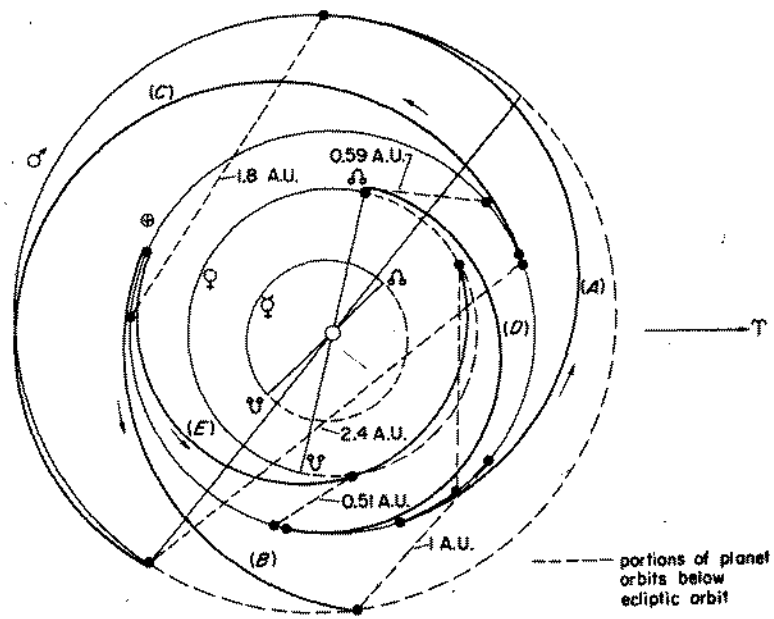

FIG. 9-9 Effect of Departure Time on Required Transfer Orbit and Distance from Earth Upon Arrival at Target Planet.

distance from the Earth, at arrival Mars, is very large (1.8 A.U.). A shorter transfer orbit, such as (B), is therefore very desirable and, for smaller instrumented payloads practically mandatory, for reasons of data transmission (i.e., power requirement as well as directional accuracy requirement of the transmitter antenna). If one wants to launch a probe to Mars at a time very much different from those given for Mars in Tab. 9-6, then a transfer orbit such as (C) may be required. Although this orbit does not require very much energy (if no Martian capture is intended; cf. below), this arrival distance from Earth is enormous. What is almost worse, Mars is close to a conjunction with the Sun. Radar transmission quality is therefore likely to be inferior. In the case of Venus the minimum energy transfer provides good transmission conditions [transfer orbit (D) which resembles the transfer orbit to Venus as it could have been flown on June 8, 1959]. Shorter transfer orbits (E) therefore do not yield the same improvement in transmission conditions as in the case of a transfer to Mars. In fact the arriving vehicle stands closer to the Sun, seen from the Earth, than in the case of the minimum energy transfer. Again for departure to Venus at a date which is considerably different from the dates given in Tab. 9-7a, a transfer orbit of the type (F) may have to be taken, resulting in considerably greater distance from Earth upon arrival. *Flexible transfer capability widens the launch window.*

Above considerations apply mainly to instrumented probes. For independent piloted space vehicles, proximity of the Earth is not required, accuracy tolerances are less critical because of superior navigational capability, and energy requirement will be comparatively less of a restriction due to the development of better propulsion systems than those which will power earlier instrumented probes. Emergency rescue missions into interplanetary space are another mission type for which few restrictions are acceptable, outside possibly of the transfer time which should be short.

9-4 COMPUTATION OF LONG AND SHORT TRANSFER ORBITS, ASSUMING CO-PLANAR CIRCULAR PLANET ORBITS

It was pointed out in the preceding paragraph that the available launch window is broadened with the availability of transfer orbits other than the Hohmann orbit. For 1-way missions, short transfer orbits are especially attractive. An extension of the allowable launching period is of particular interest for missions to Venus and Mars, because of the long synodic periods of these planets with respect to the Earth.

The computation of *short transfer orbits between circular co-planar planet orbits* is most conveniently carried out by using the apsidal distances or the heliocentric departure velocity and departure angle as independent

variables and determining the transfer time as well as other parameters of interest as function of these terms. Subsequently, a number of computation schemes will be presented for intersecting orbits.

(*I*) *Basic Assumptions*

1. The planet orbits are assumed to be circular and co-planar. Intersection angles with the transfer paths are therefore θ, defined as angle between flight direction and normal to the radius vector at the heliocentric intersection point with the target orbit.
2. Planetary fields of gravitation are neglected, except for determination of the over-all mission velocity.
3. Unit of length is the astronomical unit (A.U.), defined as the semi-major axis $a_\oplus$ of the Earth's orbit, i.e., $a_\oplus = 1.0$.
4. Unit of velocity is the circular velocity at 1 A.U. distance.
5. Unit of time is the second.
6. The above defined dimensionless distances and velocities will be designated by an asterisk.

(*II*) *Elliptic Heliocentric Transfer Orbits No. 1 and 4* (Fig. 9-10, Fig. 9-11)

Departure from R^*_P R^*_A

Independent variable R^*_A R^*_P

Alternate independent variable $a^* = \frac{1}{2}(R^*_P + R^*_A)$

Computation:

(1) $$V^*_P = \sqrt{R^*_A/a^*} \qquad V^*_A = \sqrt{R^*_P/a^*}$$

(2) $$\pm \Delta V^*_1 = v^*_{\infty,1} = V^*_P - 1 \qquad |V^*_A - 1|$$

(3) $$e = \frac{R^*_A}{a^*} - 1 \qquad 1 - \frac{R^*_P}{a^*}$$

(4) $$\cos E_2 = \frac{a^* - a^*_{\mathrm{pl}}}{a^* e} \qquad -\frac{a^* - a^*_{\mathrm{pl}}}{a^* e}$$

(5) Eccentric anomaly = E_2 (deg) $\quad 180 - E_2$ (deg)

(6) $$M_2 \text{ (radians)} = E_2 \text{ (radians)} - e \sin E_2$$

(7) $$t_t \text{ (sec)} = M_2 \sqrt{\frac{a^{*3}}{K_\odot}} \qquad \sqrt{\frac{a^{*3}}{K_\odot}} (\pi + M_2)$$

(8a) $$\cos \eta_2 = \frac{\cos E_2 - e}{1 - e \cos E_2}, \text{ or}$$

(8b) $$\cos \eta_2 = \frac{|a^*(e^2 - 1)| - 1}{e}$$

PRINCIPLES OF
GUIDED MISSILE DESIGN

Edited by

GRAYSON MERRILL, CAPTAIN, U.S.N. (Ret.)

SPACE FLIGHT

II. DYNAMICS

KRAFFT A. EHRICKE

Director of Advanced Studies
GENERAL DYNAMICS/ASTRONAUTICS

1962

D. VAN NOSTRAND COMPANY, INC.
PRINCETON, NEW JERSEY · TORONTO · NEW YORK · LONDON